PHILOSOPHICAL TRANSACTIONS OF THE ROYAL SOCIETY B BIOLOGICAL SCIENCES

# Silica Deposition and Ultrastructure in the Cell Wall of Equisetum arvense: The Importance of Cell Wall Structures and Flow Control in Biosilicification?

C. C. Perry and M. A. Fraser

*Phil. Trans. R. Soc. Lond. B* 1991 **334**, 149-157
doi: 10.1098/rstb.1991.0104

# Silica deposition and ultrastructure in the cell wall of *Equisetum arvense*: the importance of cell wall structures and flow control in biosilicification?

C. C. PERRY AND M. A. FRASER

*Chemistry Department, Brunel University, Uxbridge, Middlesex UB8 3PH, U.K.*

## SUMMARY

Scanning and transmission electron microscopy have been used in the investigation of the surface micromorphology and ultrastructure of silicas extracted from different regions of the horsetail *Equisetum arvense*. The surface micromorphology was found to be very complex and varied with the anatomical region of the plant. Principally fibrillar, globular and sheet-like ultrastructural motifs of silica were observed, their proportions and detailed structure also varying with the anatomical region studied. The physiocochemical mechanisms by which these structural motifs arise are discussed in relation to the surface micromorphologies observed and to their anatomical function.

## 1. INTRODUCTION

Although silicification of plants was first reported by de Saussure in 1804 (see Jones & Handreck 1967) it still remains a phenomenon which is not widely acknowledged and is poorly understood.

Silica is deposited in a wide variety of taxa among vascular plants (Parry *et al.* 1984) with monocotyledons being the heavier accumulators. Horsetails in particular accumulate more than 25% of their dry mass as silica and have been shown to require silicon as an essential element for growth (Chen & Lewin 1969).

All biogenic silicas formed *de novo* are non-crystalline (Mann & Perry 1986) and the term amorphous silica encompasses a wide variety of structural forms from ordered particulates to extended gel-like materials, and as such, biogenic silica is not a stoichiometric mineral. The nature and composition of biological siliceous structures can be extremely variable, being influenced directly and indirectly by a wide variety of cellular processes.

A wide variety of techniques are available for the study of biogenic silicas (Perry 1989; Webb & Perry 1989) depending upon the level of chemical and structural information required. A sophisticated battery of techniques including solid $^{29}$Si nuclear magnetic resonance (NMR) infrared spectroscopy, electron microscopy and surface analysis are necessary for characterization at the molecular, microscopic and macroscopic levels.

Characterization of silica from the macrohairs of *Phalaris canariensis* L. has shown that different ultrastructures, identified by fundamental particle size and orientation (Perry *et al.* 1984) and surface functionality (Perry *et al.* 1990), occur in different cell wall regions and are deposited at different stages of development (Hodson *et al.* 1984; Perry *et al.* 1984*a*, *b*, 1987). In addition, the ultrastructural forms observed, namely globular, sheet-like and fibrillar, could be related to changes in synthesis of cell wall polymers (Perry *et al.* 1987).

Scanning electron microscopy coupled with electron microprobe analysis has been extensively used to study silica distribution in grasses (Kaufman *et al.* 1972; Hayward & Parry 1973; Dinsdale *et al.* 1979), nettle stinging hairs (Thurston 1974), sugar cane (Sakai & Thom 1979) and horsetails (Kaufman *et al.* 1971; Page 1972). In contrast to the generalized distribution of silica demonstrated in most grasses, that of the horsetails is highly individual and surface sculpturing of silica papillae and rosettes have been used as an aid to classification within the subgenus *Equisetum*. However, the above studies have neither considered the microscopic nature of the silica utilized in the formation of macroscopic structures such as papillae, or considered the relation of the observed silica deposits to either transpiration or cell wall composition.

This paper presents information obtained from the study of silicas extracted from different anatomical regions of the aerial shoots of *Equisetum arvense*. The importance of structure–function relation, cell wall composition and transpiration in the development of specific silicified structures is discussed.

## 2. MATERIALS AND METHODS

Samples of sterile shoots of *Equisetum arvense* (source; Wytham Woods, Oxford and Royal Holloway and Bedford New College, Egham) were harvested in late spring and early autumn before branching.

Shoots were separated into: (i) stem nodes; (ii) stem internodes; (iii) basal branches; (iv) distal branches and (v) leaves. Samples were dried at room temperature and lightly ground with a pestle and mortar

*Phil. Trans. R. Soc. Lond.* B (1991) **334**, 149–157
*Printed in Great Britain*

before treatment with a mixture of concentrated nitric and sulphuric acids (4:1 by volume) heated at 100 °C for at least 24 h to remove the organic cell wall components until less than 0.1 % carbon remained in the samples as detected by gas chromatography.

Samples (intact and acid treated) were mounted on aluminium stubs using M-glue (Agar aids) and coated with carbon for analysis by scanning electron microscopy (SEM) in a JEOL 840 SEM operating at a beam voltage of 3–15 keV† and a working distance of 13–25 mm.

Samples for study by transmission electron microscopy (TEM) were finely ground using a pestle and mortar, suspended in acetone, and drops of the suspension were dried onto holey carbon, formvar-coated electron microscope grids and examined in a JEOL 2000FX electron microscope operating at 200 keV.

The data presented in this paper derive from an extensive study of immature and mature, intact and acid-treated material. Representative micrographs only are presented in the figures.

Figures 1–13 refer to SEM data obtained from mature acid-treated samples. Long arrows on figures 2, 5, 6, 7, 9 and 10 indicate the axis of the stem node, internode or branch respectively. Short arrows indicate points of interest as outlined in the text. p, pilulae; r, rosette; m, mamilla; s, stomata; R, ridge; G, groove.

Figures 15–22 refer to TEM data obtained from acid-treated samples. Where structures were virtually identical for different anatomical regions only one example is shown. In many instances, structural motifs were more clearly observed from immature samples (layers of silica were packed less densely) and these have been chosen to illustrate the structural motifs observed. All scale bars represent 200 nm.

## 3. RESULTS

It is noted that removal of the organic cell wall components led to a clearer definition of siliceous structures, suggesting that at the epidermal surface the organized silica structures are overlayed by only a thin layer of organic material which somewhat masks the micromorphological relief observed. Little degradation in morphological structure was observed for acid-treated samples, and results show that, for this system, silica is an important component of almost all cell wall components. All figures shown comprise silica only.

Inner, fractured surfaces after removal of the organic cell wall components revealed the distribution of silica within the cell wall to be exclusively within the secondary cell wall (figure 1). No silica was found to be present in the middle lamella, or in areas where plasmodesmata or other intracellular communication sites were located. Thus it can be inferred that silica in the cell walls of *Equisetum arvense* is not complexed or associated with the pectic cell wall polysaccharides that are prominent in the middle lamella.

## 4. SURFACE MORPHOLOGICAL STUDIES

Most of this study was involved with the relation of surface micromorphology to silica ultrastructure at the nanometre level. For the five samples studied (intact and acid treated), clear distinctions were observed between the branch portions and the stem node, internode and leaf regions. However, both the distal and proximal branch portions were essentially similar with respect to surface micromorphological features observed. In a morphological study by Page (1972), 12 characteristics were used to describe the nature of the surface features observed. In this paper, a similar classification has been adopted and detailed descriptions of each anatomical region studied are given.

The stem internode and node appear structurally very similar. Both are characterized by wide fairly shallow grooves flanked by narrow ridges (figure 2). Stomata were located along the flanks of the grooves and were not normally seen to be inclined with respect to the groove axis. Stomata were widely spaced, normally forming a single row along the groove flank, and were located in distinct depressions formed by adjacent epidermal cells. Stomata had an approximately circular plan and the companion cells had a low convex profile (figure 3). The periphery of the stomatal apparatus was defined by a distinct single row of bead-like pilulae. The pilulae covering the companion cells were small and ranked in rows running the

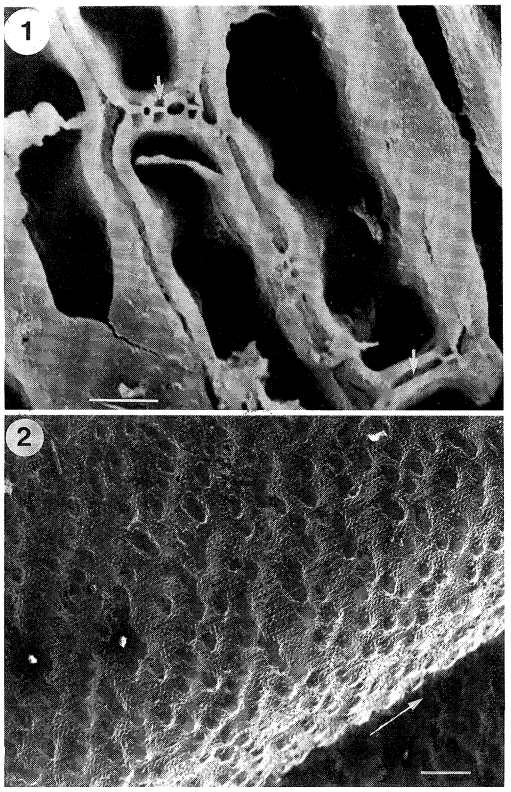


Figure 1. Inner fractured nodal surface where epidermal cells are viewed in longitudinal section. Silica is not located within the middle lamella and primary wall or at points of cell–cell connection (arrowed). Scale bar represents 10 μm.

Figure 2. Internodal groove with aligned rows of pilulae running parallel to the internodal axis. These are sometimes disrupted by discrete, convex, unadorned mamillae which occasionally fuse to form bars perpendicular to the internodal axis. Scale bar represents 100 μm.

† 1 eV ≈ $1.602 \times 10^{-19}$ J.




PHILOSOPHICAL TRANSACTIONS OF THE ROYAL SOCIETY B BIOLOGICAL SCIENCES

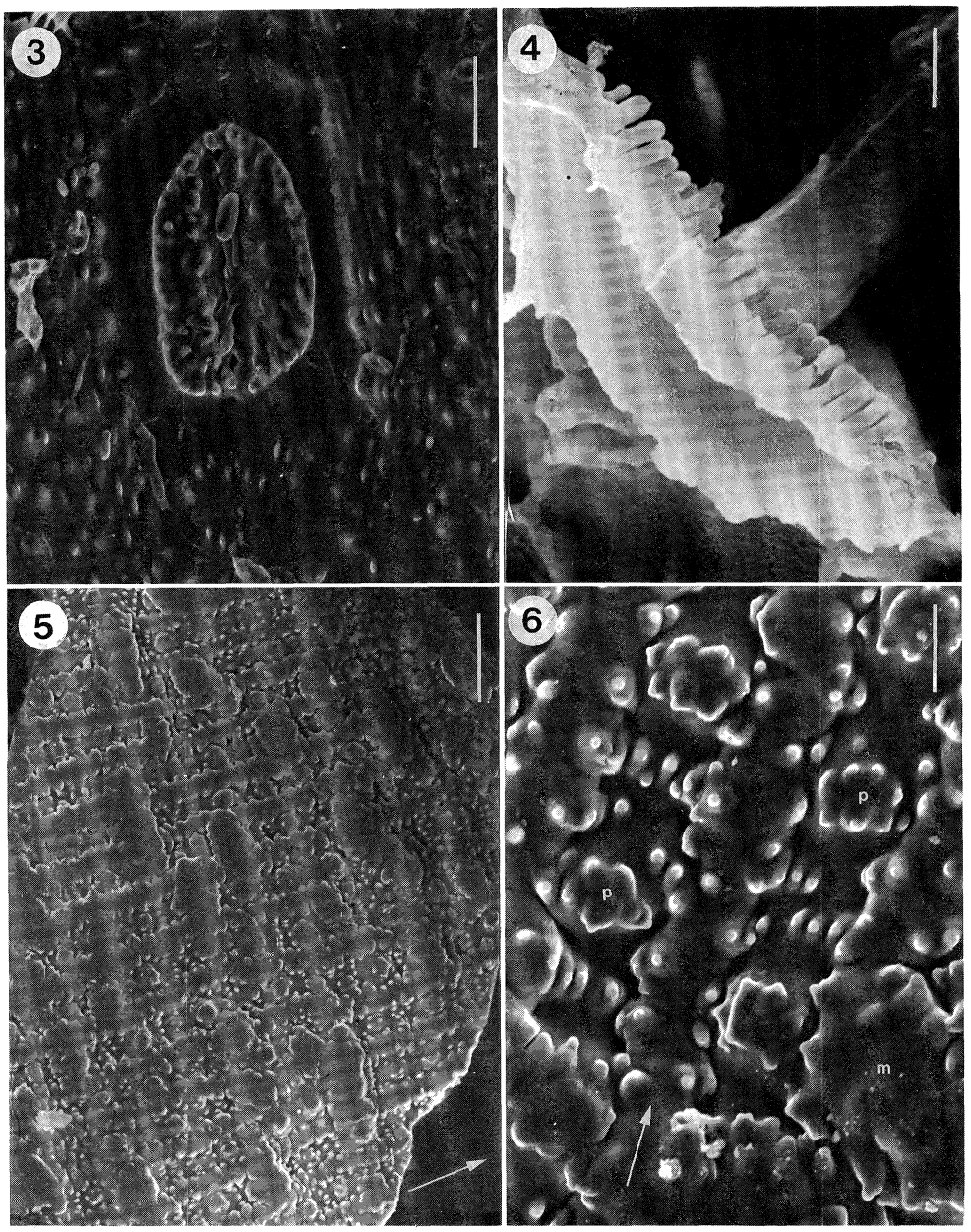


Figure 3. Stomatal apparatus from the internode. The stomatal apparatus is sited in a distinct depression delineated by an irregular row of pilulae. The companion cells have a low convex profile and an approximately circular plan. Scale bar represents 20 μm.

Figure 4. Fractured cross-sectional view of a stomatal companion cell showing elongated ranks of pilulae along the stomatal surface. Scale bar represents 10 μm.

Figure 5. Surface sculpturing of a node groove with aligned rows of pilulae running parallel to the principal axis of the plant. The pilulae often fuse to form narrow ridges (arrowed) disrupted by extensively fused mamillae having an irregular low convex profile. Scale bar represents 50 μm.

Figure 6. Nodal groove region showing parallel fused rows of pilulae (arrowed), separated by individual fused clusters of pilulae and further disrupted by large irregular mamillae Scale bar represents 10 μm.

length of the cells, and became progressively more elongated towards the stomatal aperture (figure 4).

The epidermal cells of the groove were covered by distinct tramline-like paired rows of pilulae that were periodically disrupted by large irregular and flattened mamillae that were aligned transversely across the groove and were often seen to fuse with adjacent mamillae to form discrete bars (figure 5). This was particularly noticeable in the node region, where there was often little space between adjacent transversely orientated bars. Also, individual pilulae were often seen to fuse with adjacent rows to form bars running parallel to the stem axis (figure 6).

The node and internodal ridges were often heavily encrusted with pilulae, sometimes aligned into rows and sometimes randomly distributed, and the ridge crests were often covered by a continuous row of mamillae variably encrusted with pitulae. This was particularly obvious in the node region, where there was no obvious distinction between the ridge and

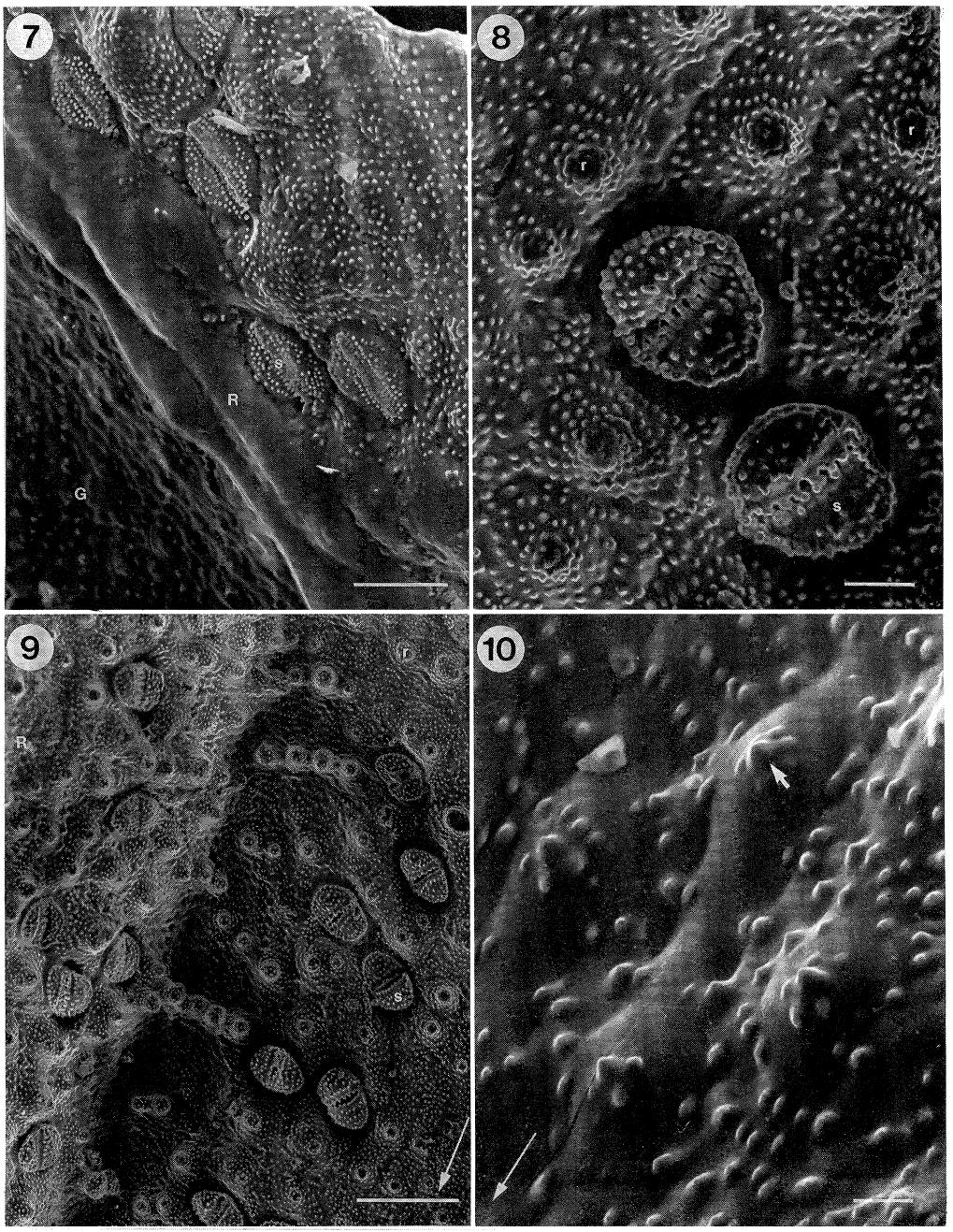


Figure 7. Basal portion of branch showing distinct ridge and groove pattern. Stomata are aligned in double offset rows running along the groove flank in distinct depressions formed by adjacent epidermal cells and topped by convex mamillae encrusted with conical pilulae and rosettes. Stomata were covered by rows of pilulae which became elongated and dumb-bell shaped towards the stomatal openings. Ridge cells are elongated and devoid of pilular encrustation. Scale bar represents 50 μm.

Figure 8. Stomatal apparatus from the distal portion of the branch showing the high convex profile of the companion cells covered with parallel rows of pilulae which become increasingly elongated and dumb-bell shaped towards the stomatal aperture. Scale bar represents 20 μm.

Figure 9. Groove flank from the basal portion of the branch showing double offset rows of stomata inclined with respect to the groove axis. Adjacent epidermal cells are heavily encrusted by pilulae and mamillae surmounted by ornate rosettes which often fuse to form bars. Scale bar represents 100 μm.

Figure 10. Epidermal ridge cells from the basal portion of the branch which are only lightly encrusted with pilulae but surmounted by single rosettes. Scale represents 50 μm.

groove surface micromorphology (figure 5). The pilulae covering the groove flanks had a conical appearance whereas those on the ridge and groove had a more rounded appearance.

The leaves, which formed a toothed sheath around the node, were found to be morphologically very similar to the internode. However, the level of surface organization was somewhat lower than in the internode. That is, the pilulae were not as rigidly organized into tramline-like rows, mamillae were smaller and less




PHILOSOPHICAL TRANSACTIONS OF THE ROYAL SOCIETY B BIOLOGICAL SCIENCES

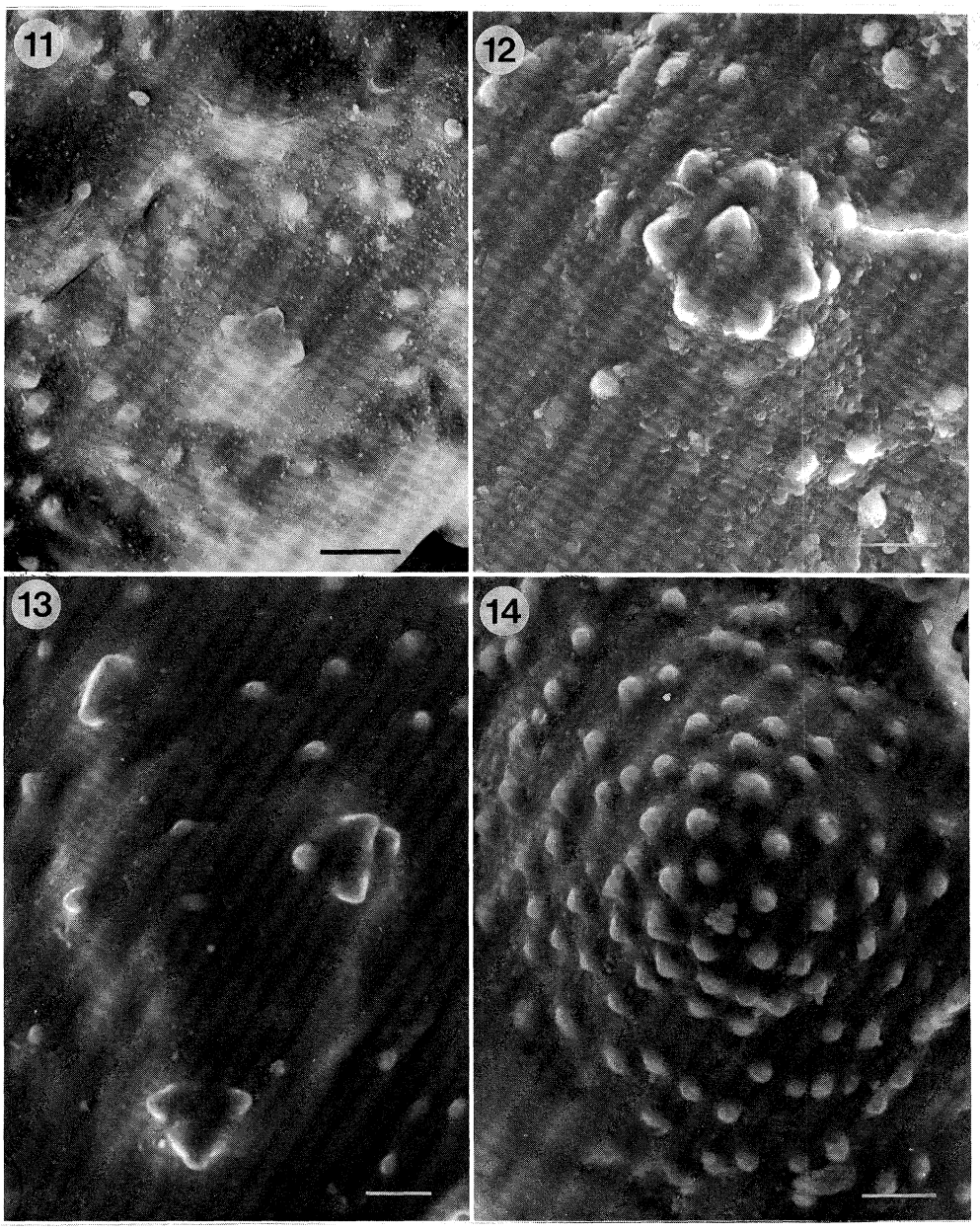


Figures 11–14. Pilulae found in the groove flank region of the branches showing a range of cluster and star-like aggregates. Scale bars represent 1 μm.

clearly defined, and the pilulae covering the stomatal companion cells were simple and not elongated.

The basal and distal portions of the branches were morphologically very similar but were quite distinct from the other parts of the plant. The most obvious feature was the longitudinal ribbing of the branches. However, the ribs on the branches were much narrower and the grooves deeper than on the stem. Stomata were located on the flanks of the grooves, transversely aligned in groups of two to four and inclined with respect to the axis of the branch (figure 7). Pilulae covering the companion cells were elongated, dumb-bell shaped and intermeshed at the stomatal aperture. Stomata were located in shallow depressions delineated by an irregular row of pilulae (figure 8).

The epidermal cells in the region of the groove flanks were surmounted by regular clusters of conical pilulae in the form of star-shaped rosettes or clusters (figures 11–14) that were often seen to fuse to form bars (figure 9). The remainder of the epidermal cells were covered by a random dispersion of bead-like pilulae.

The epidermal cells of the ridges were surmounted by a continuous row of mamillae and were normally devoid of any pilular encrustation (figure 10). Occasionally, however, individual cells were seen to be topped by one or two five- or six-pointed star-shaped rosettes. The epidermal groove cells were normally covered by a random dispersion of pilulae although sometimes organization into tramline-like double rows was seen, and occasionally further organization into groups of rows, only occasionally disrupted by irregular flattened mamillae, with irregular pilular encrustation.

## 5. ULTRASTRUCTURAL STUDIES

TEM was used to identify the nature of the ultrastructural motifs used to form the macroscopic features observed in the scanning microscopy study. Images

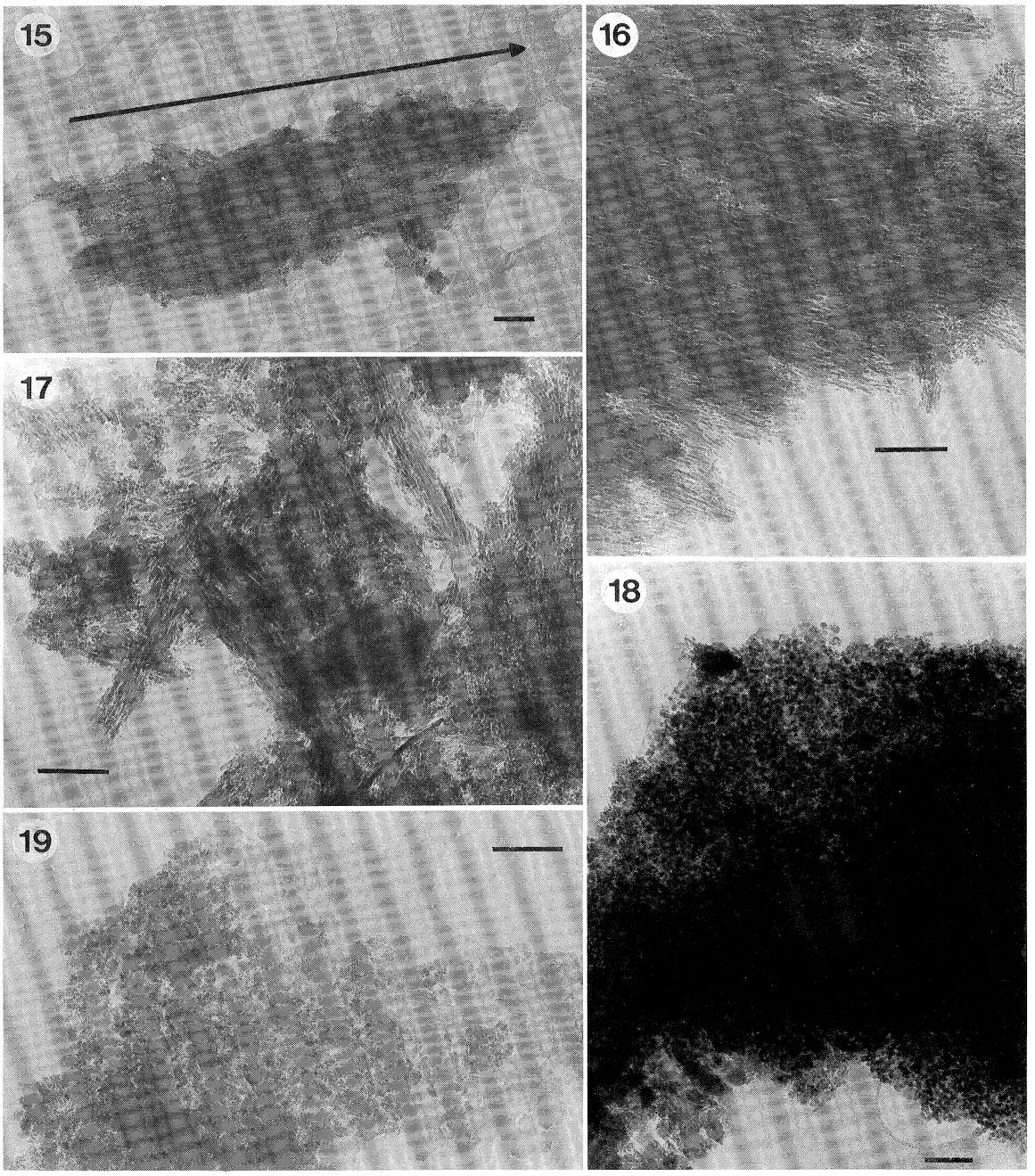


Figure 15. Fibrillar silica from a mature internode. The material is oriented with the principal axis of the plant.

Figure 16. Fibrillar silica from an immature internode showing clear orientation and dense packing of the individual fibrils.

Figure 17. Small regions of fibrillar material showing random orientation and some sheet-like silica.

Figure 18. Silica from a node showing densely packed sheets of globular material.

Figure 19. Immature node showing some particulate material and structurally indistinct beam-sensitive material.

observed were classified according to particle size, relative orientation, size of area of a particular ultrastructural type, beam stability and density of packing. All three ultrastructural forms of silica observed in the study of macrohairs from *Phalaris canariensis* L. (Perry *et al.* 1984) were also observed in this study. However, the relative proportions of the basic individual globular, fibrillar and sheet-like structural motifs was found to vary with sample age and the anatomical origin of the sample. It is noted that, in general, particulate structures were built up from particles of regular size and showed little evidence of 'Ostwald ripening'.

Analysis of silica deposits extracted from the node and intermodal regions of the stem of *Equisetum arvense* revealed these to be ultrastructurally similar for both the immature and mature samples. They were, however, ultrastructurally distinct from the branch samples described below.

In mature samples of the stem internode the most significant feature was the amount of highly organized and densely packed fibrillar material (figure 15). Each




PHILOSOPHICAL TRANSACTIONS OF THE ROYAL SOCIETY B BIOLOGICAL SCIENCES

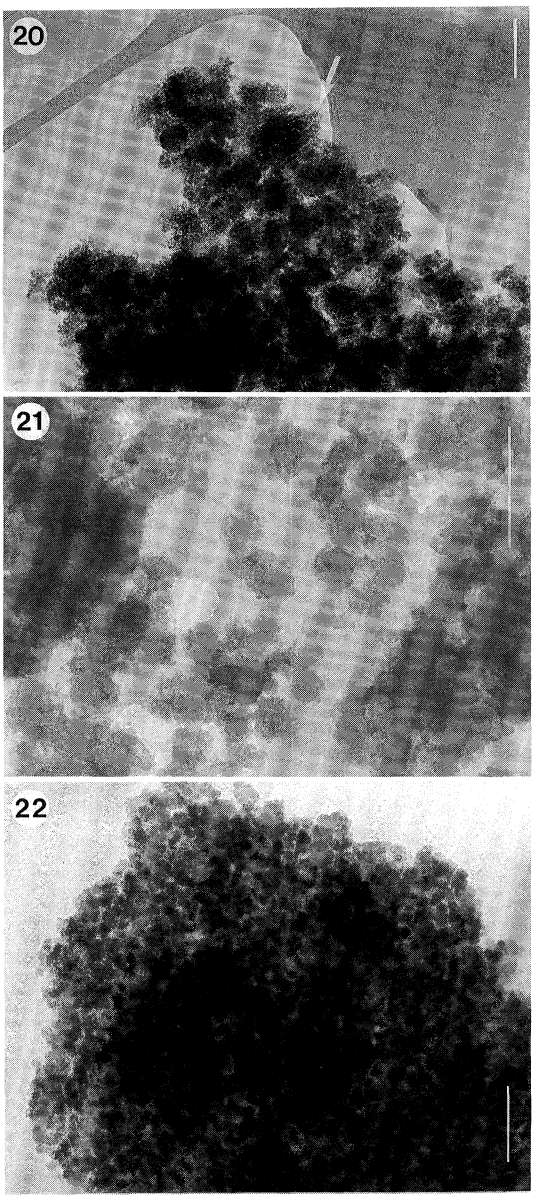


Figure 20. Globular material and small areas of oriented material (arrowed) from the branches.

Figure 21. Beam-sensitive globular material from immature branches.

Figure 22. Globular silica from the branches.

fibrillar sheet was composed of parallel fibrils, each formed from individual lozenge-shaped particles measuring approximately 5 nm × 3 nm. The fibrillar arrays appeared to be sandwiched together to give thick areas of material with uniform orientation (figure 16). Other less extensive fibrillar arrays were observed, composed of small individual fibrillar sheets having either a uniform orientation or random orientation forming a mesh-like array (figure 17). These extensive fibrillar arrays were interspersed with areas of densely packed globular sheeting composed of clusters 70–150 nm in diameter and built up from individual silica particles of about 7–8 nm in diameter (figure 18). The immature internode was characterized by extensive arrays of fibrillar sheeting showing both types of arrangement, namely directionally-oriented sheets or random orientational arrangements, although the preponderance of the latter was higher than for the mature samples. In addition, large amounts of structurally indistinct beam-sensitive material was also observed (for example see figure 19. In many respects, the immature internodal silica was quite similar to that observed for the mature node, although it contained less fibrillar material and the density of packing of the particles and sheets was significantly reduced. In the node, the presence of overlapping randomly oriented fibrillar material was more evident, interspersed with regions of globular material. Clusters of particles were again of variable size and were less densely packed than in the internode, and a significant increase in the structurally indistinct phase was observed. The immature node was characterized by a reduction in the amounts of fibrillar material and by a decrease in packing density for the other structural motifs.

Silica deposits extracted from the leaves of *Equisetum arvense* were found to be ultrastructurally very similar to those found in the node and internode, and comprised primarily fibrillar material organized into overlapping sheets of fibrils with virtually identical orientation. Smaller sheets of fibrillar material showing little intersheet orientation and interspersed with globular material were also observed. The size of the particles and their stability with respect to the electron beam were consistent with those found in the node and internode.

Branch samples were built up from large areas of globular material (figure 22). Individual particles were 7–8 nm in diameter and the primary clusters 50–180 nm in diameter. The density of packing of these particles was high although samples exhibited poor beam stability, suggesting that the samples were hydrated. In addition, small areas of fibrillar material, normally no larger than 300 nm × 150 nm were sometimes observed interspersed with the globular matrix. Particles were arranged in short parallel rows (figure 21). Immature samples from the branches were ultrastructurally very similar to the mature samples, although the density of packing of the globular particles was lower and the proportion of material significantly less stable in the electron beam higher, suggesting an increased level of hydration of the silica phase (figure 20).

## 6. DISCUSSION

The results presented above clearly show differences between the different anatomical regions of *Equisetum arvense*, both in terms of surface micromorphological sculpturing and in the ultrastructural form that the particulate silica adopts. It is thought that the predominant ultrastructural silica motif for a particular anatomical region could be related to the surface micromorphology observed, and that this could be related to the role of that particular part of the plant in relation to the whole.

The micromorphological survey showed considerable variation in the surface relief of the distinct anatomical regions studied, and although these features appear not to be of taxonomic importance they are clearly important to the function of the plant.




PHILOSOPHICAL TRANSACTIONS OF THE ROYAL SOCIETY B BIOLOGICAL SCIENCES

The ultrastructural silica motifs exhibited by a particular anatomical sample were found to correspond well to the surface micromorphology observed for that sample. That is, the silica extracted from the mature node, internode and leaf samples was found to be ultrastructurally very similar, consisting predominantly of highly organized fibrillar sheets, either having the same fibrillar orientation as was found chiefly in the internode, or of multiple fibrillar orientation as was found in the node.

The basal and distal portions of the branches were found to be built up from essentially only globular material, which was more susceptible to beam damage and was more heavily hydrated. The section of the branches closest to the stem contained more fibrillar material than sections further from the stem.

It is suggested that the ultrastructural motifs observed are directly related both to the surface micromorphology and to the functioning of the different anatomical regions of the plant. In the case of the internode and node, the predominant function is the maintenance of mechanical strength and rigidity. This can readily be achieved by having a highly directionally organized network of fibrillar sheets intermeshed with the organic cell wall polymers. The structure of the fibrillar silica motif may be controlled by the cellulose microfibrillar network acting as a template for silica deposition. Note the preponderance of silica oriented with the principal axis of the plant found in the internodal regions and the presence of randomly oriented fibrillar silica in the nodal regions. It is suggested that the fibrillar silica promotes mechanical strength, the presence of multioriented material providing, in addition, rigidity to overcome the stresses of water flow etc. In addition, the silica bars that are so dominant in the node and to a lesser extent in the internode also have a functional role, and at the micromorphological level reflect the underlying ultrastructure of the siliceous phase.

In the branches, where mechanical rigidity is of less importance and the ability to overcome stresses induced by wind action becomes desirable, the presence of bars arising from the fusion of adjacent mamillae is absent. Surface ornamentation on the branches is, however, complex with the presence of highly ornate silica rosettes. These are clearly of little mechanical significance although they may be the means by which *Equisetum arvense* gains protection against attack by insect predators. It is thought that the large, angular silica encrustations may render the otherwise more delicate branches unpalatable to predators. The high proportion of globular silica and concomitant decrease in fibrillar silica correlates well with the increase in surface ornamentation (bead-like pilulae and rounded mamillae) and the decline in importance of the structural role played by the silica in the branches.

An additional means of defence against pathogenic organisms is provided by the dumb-bell shaped interlocking pilulae at the stomatal apertures, and it is likely that these are also built up from principally globular material.

Model precipitation studies (Perry & Lu 1991) have shown that both the polymerization and aggregation processes of silica deposition can be directed by carbohydrate polymers. Hemicelluloses in solution affect initial polymerization rates but have little or no effect on aggregation. Polymers such as cellulose, however, show significant effects on particle growth and aggregation although there is no effect on the initial stages of polymerization. The presence of cellulose in the reaction media was observed to orient regularly-sized particles into sheet-like arrays and prevent 'Ostwald ripening'. It is indeed likely that the three-dimensional characteristics of polymer surfaces direct and control aggregation characteristics such that the structures observed in biology may 'faithfully' represent the texture of the filamentous structure of the cell wall.

In addition, the structural motifs observed in the different regions of the aerial shoots of *Equisetum arvense* give circumstantial evidence for the involvement of water transport in the formation of structural motifs. In the stem, where water flow is greatest, the principal structural motif observed is the fibrillar motif. At the ends of the leaves, where water flow is expected to be least (most stomata are found on the stem), principally globular material is found. In addition for the leaf sections nearest the stem, a small proportion of fibrillar material is observed. It is possible that the fundamental silica particles are not formed *in situ* but are nucleated within the transpiration stream and transported to their final site before they ripen. The size of the particles may in part be governed by conditions within the transpiration stream (for example, pH, silicon concentration, inorganic and organic, ionic and uncharged, species at variable concentrations) as well as the composition of the organic matrix into which the particles are forced by the slow flow of fluid. The shapes and biochemical characteristics of the individual cells within the stems and branches, as well as the importance of water flow, may be important factors in determining the morphologies observed in such a primitive plant.

Overall, the surface micromorphology of the stem internode and leaves have been shown to be very similar to those described in the taxonomic survey by Page (1972). However, this study has revealed marked differences in the surface micromorphology of the anatomically distinct regions of *Equisetum arvense* and has correlated these with differences in the level of organization of silica at the ultrastructural level. In this and other heavily silicified systems the silica acts as an *in vivo* stain, faithfully reproducing the organic matrix skeleton at the microscopic and macroscopic levels without staining.

This work was funded by the AFRC.

## REFERENCES

Chen, C. & Lewin, J. 1969 Silicon as a nutrient for *Equisetum arvense*. *Ann. Bot.* **47**, 125–131.

Dinsdale, D., Gordon, A. H. & George, S. 1979 Silica in the mesophyll cell walls of Italian Rye grass (*Lolium multiflorum* Lam. cv. RVP) *Ann. Bot.* **44**, 73–77.

Hayward, D. M. & Parry, D. W. 1973 Electron-probe





PHILOSOPHICAL TRANSACTIONS OF THE ROYAL SOCIETY B BIOLOGICAL SCIENCES

microanalysis studies of silica distribution in Barley (*Hordeum sativium* L.) *Ann. Bot.* **37**, 579–591.

Hodson, M. J., Sangster, A. G. & Parry, D. W. 1984 An ultrastructural study of the development of silicified tissues in the lemma of *Phalaris canariensis L. Proc. R. Soc. Lond.* B**222**, 413–425.

Jones, L. H. P. & Handreck, K. A. 1967 Silica in soils, plants and animals. *Adv. Agron.* **19**, 107–149.

Kaufman, P. B., Bigelow, W. C., Schmid, R. & Ghosheh, N. S. 1971 Electron microprobe analysis of silica in epidermal cells of *Equisetum Am. J. Bot.* **58**, 309–316.

Kaufman, P. B., LaCroix, J. D., Rosen, J. J., Allard, L. F. & Bigelow, W. C. 1972 Scanning electron microscopy and electron microprobe analysis of silicification patterns in inflorescence bracts of *Avena sativa. Am. J. Bot.* **59**, 1018–1025.

Mann, S. & Perry, C. C. 1986 Structural aspects of biogenic silica. In *Silicon biochemistry CIBA Found. Symp.* **121**, pp. 40–58.

Page, C. N. 1972 An assessment of inter-specific relationships in *Equisetum* subgenus *Equisetum. New Phytol.* **71**, 355–369.

Parry, D. W., Hodson, M. J. & Sangster, A. G. 1984 Some recent advances in studies of silicon in higher plants. *Phil. Trans. R. Soc. Lond.* B**304**, 537–549.

Perry, C. C., Mann, S. & Williams, R. J. P. 1984*a* Structural and analytical studies of the silicified macrohairs from the lemma of the grass *Phalaris canariensis* L. *Proc. R. Soc. Lond.* B**222**, 427–438.

Perry, C. C., Mann, S., Williams, R. J. P., Watt, F., Grime, G. W. & Takacs, J. 1984*b* A scanning proton microprobe study of macrohairs from the lemma of the grass *Phalaris canariensis* L. *Proc. R. Soc. Lond.* B**222**, 439–445.

Perry, C. C., Williams, R. J. P. & Fry, S. C. 1987 Cell wall biosynthesis during silicification of grass hairs. *J. Plant Physiol.* **126**, 437–448.

Perry, C. C. 1989 Chemical studies of biogenic silica. In *Biomineralisation, chemical and biochemical perspectives.* (ed S. Mann, J. Webb & R. J. P. Williams), pp. 223–256. New York: V.C.H. Publishers.

Perry, C. C., Moss, E. J. & Williams, R. J. P. 1990 A staining agent for biological silica. *Proc. R. Soc. Lond.* B**241**, 47–50.

Perry, C. C. & Lu, Y. 1991 The preparation of silicas from silicon complexes: the role of polysaccharides in polymerisation and aggregation control. *J. chem. Soc. Faraday Trans.* (In the press.)

Sakai, W. S. & Thom, M. 1979 Localisation of silicon in specific cell wall layers of the stomatal apparatus of sugar cane by use of energy dispersive X-ray analysis. *Ann. Bot.* **44**, 245–248.

Thurston, E. L. 1974 Morphology, fine structure and ontogeny of the stinging emergence of *Urtica dioica. Am. J. Bot.* **61** (8), 809–817.

Webb, J. & Perry, C. C. 1989 Proton beam analysis in studies of composite biominerals. In *Biomineralisation, chemical and biochemical perspectives* (ed. S. Mann, J. Webb & R. J. P. Williams), pp. 461–490 New York: V.C.H. Publishers.

*Received 15 June 1991; accepted 22 July 1991*





PHILOSOPHICAL TRANSACTIONS OF THE ROYAL SOCIETY B BIOLOGICAL SCIENCES

PHILOSOPHICAL TRANSACTIONS OF THE ROYAL SOCIETY B BIOLOGICAL SCIENCES

gure 1. Inner fractured nodal surface where epidermal ls are viewed in longitudinal section. Silica is not located thin the middle lamella and primary wall or at points of l–cell connection (arrowed). Scale bar represents 10 μm.

gure 2. Internodal groove with aligned rows of pilulae nning parallel to the internodal axis. These are sometimes rupted by discrete, convex, unadorned mamillae which casionally fuse to form bars perpendicular to the internodal is. Scale bar represents 100 μm.

PHILOSOPHICAL TRANSACTIONS OF THE ROYAL SOCIETY B BIOLOGICAL SCIENCES

gure 3. Stomatal apparatus from the internode. The stomatal apparatus is sited in a distinct depression delineated an irregular row of pilulae. The companion cells have a low convex profile and an approximately circular plan. ale bar represents 20 μm.

gure 4. Fractured cross-sectional view of a stomatal companion cell showing elongated ranks of pilulae along the matal surface. Scale bar represents 10 μm.

gure 5. Surface sculpturing of a node groove with aligned rows of pilulae running parallel to the principal axis of e plant. The pilulae often fuse to form narrow ridges (arrowed) disrupted by extensively fused mamillae having an egular low convex profile. Scale bar represents 50 μm.

gure 6. Nodal groove region showing parallel fused rows of pilulae (arrowed), separated by individual fused clusters pilulae and further disrupted by large irregular mamillae Scale bar represents 10 μm.


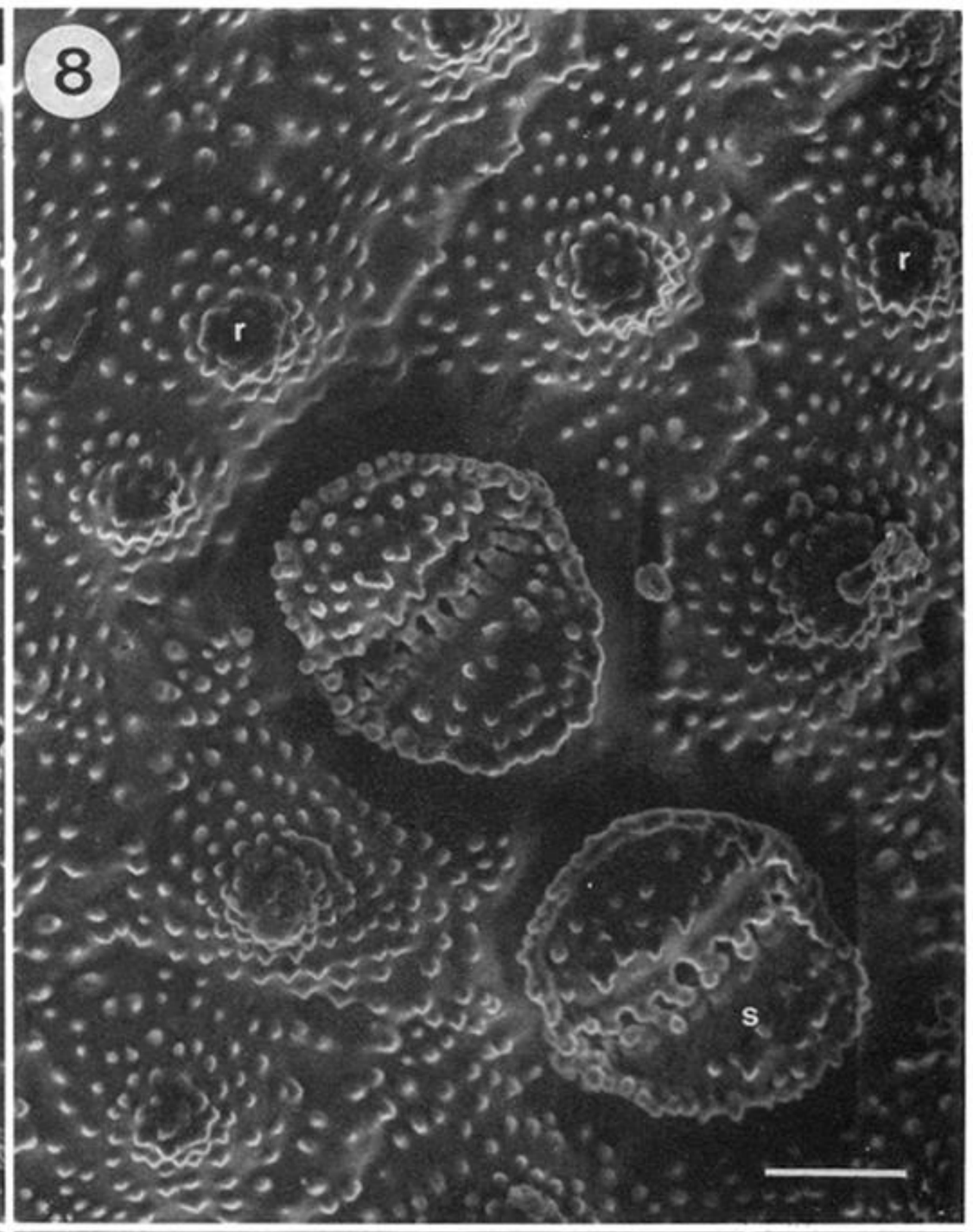


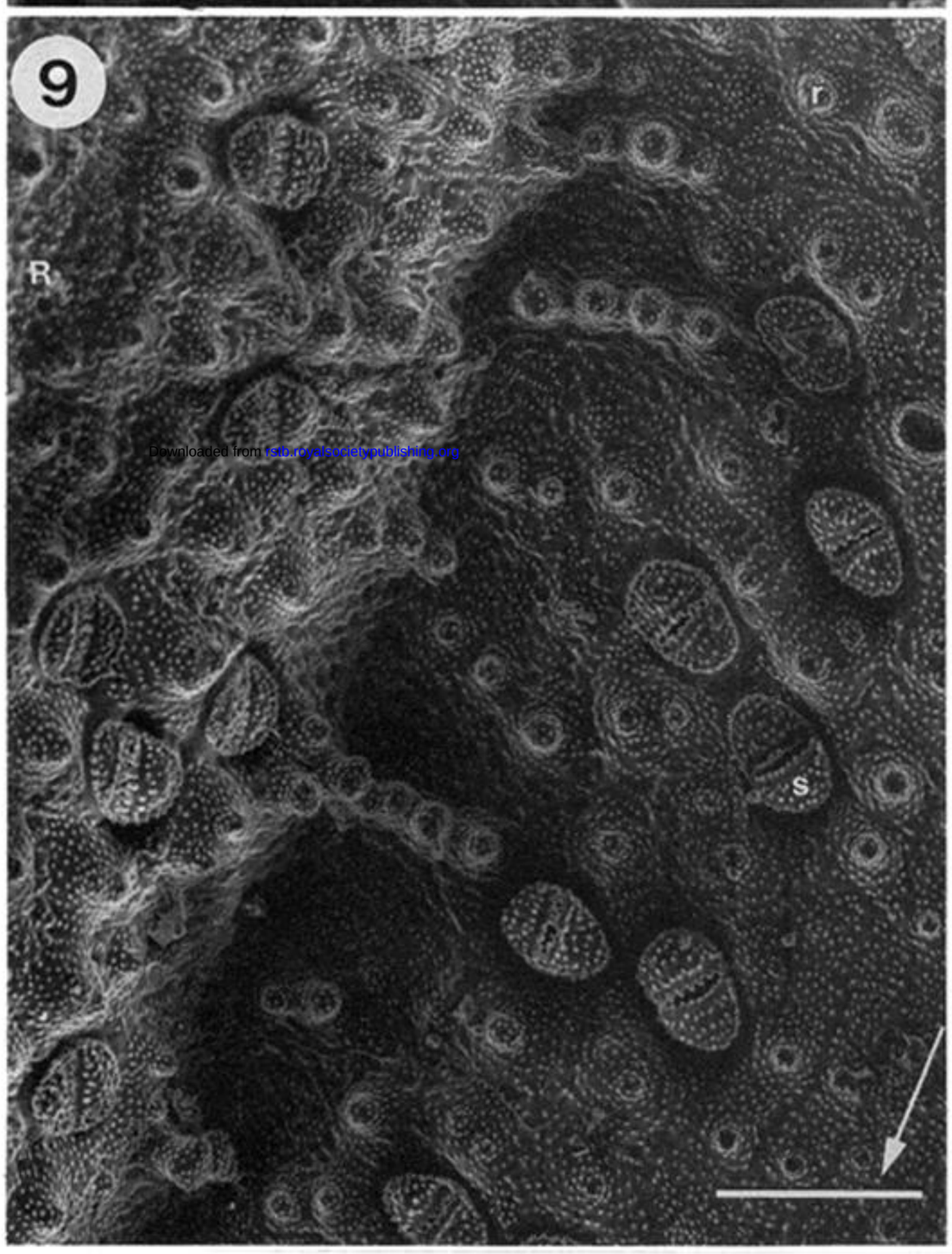


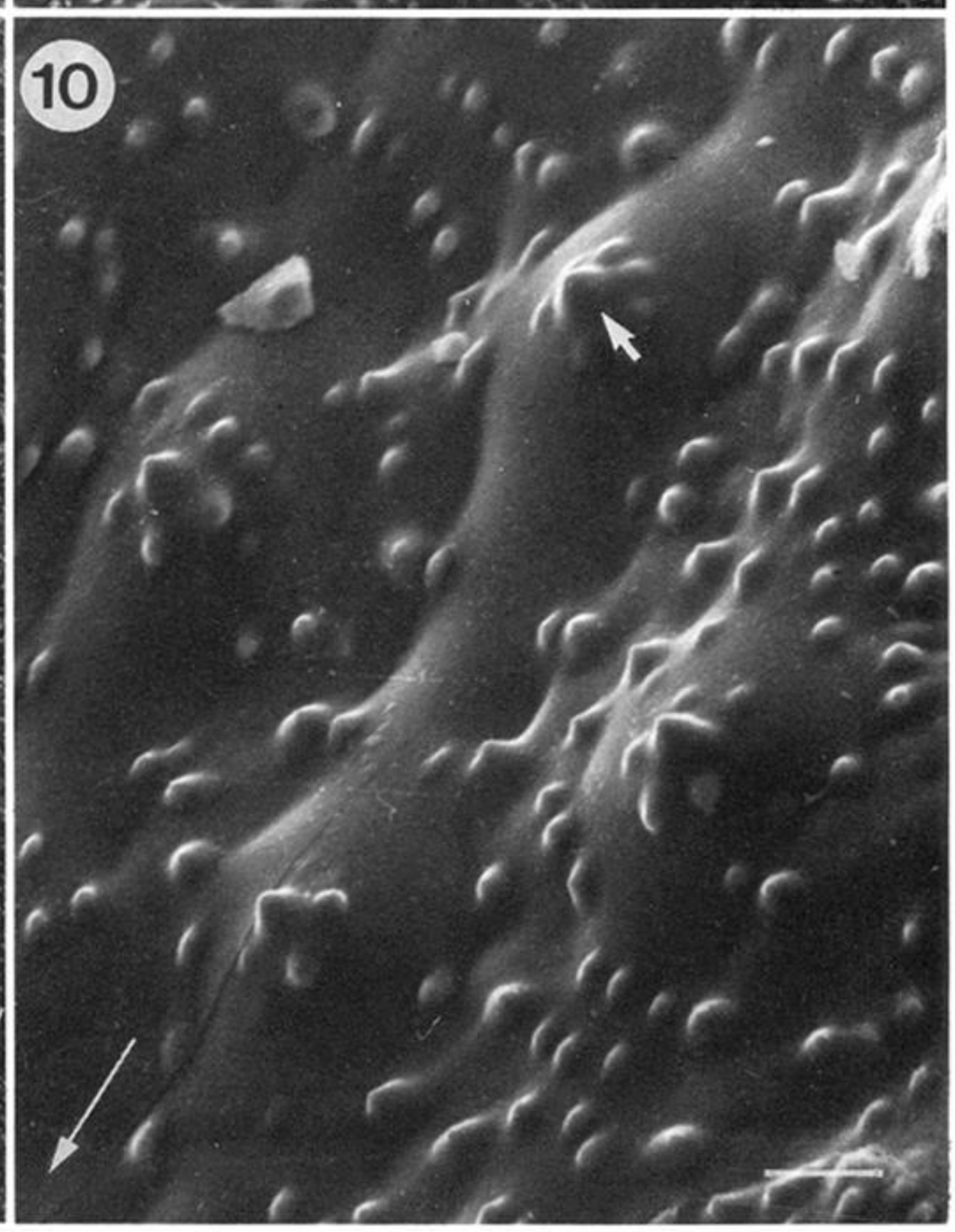






gure 7. Basal portion of branch showing distinct ridge and groove pattern. Stomata are aligned in double offset ws running along the groove flank in distinct depressions formed by adjacent epidermal cells and topped by convex amillae encrusted with conical pilulae and rosettes. Stomata were covered by rows of pilulae which became ngated and dumb-bell shaped towards the stomatal openings. Ridge cells are elongated and devoid of pilular crustation. Scale bar represents 50 µm.

gure 8. Stomatal apparatus from the distal portion of the branch showing the high convex profile of the companion ls covered with parallel rows of pilulae which become increasingly elongated and dumb-bell shaped towards the omatal aperture. Scale bar represents 20 µm.

gure 9. Groove flank from the basal portion of the branch showing double offset rows of stomata inclined with pect to the groove axis. Adjacent epidermal cells are heavily encrusted by pilulae and mamillae surmounted by nate rosettes which often fuse to form bars. Scale bar represents 100 µm.

gure 10. Epidermal ridge cells from the basal portion of the branch which are only lightly encrusted with pilulae t surmounted by single rosettes. Scale represents 50 µm.

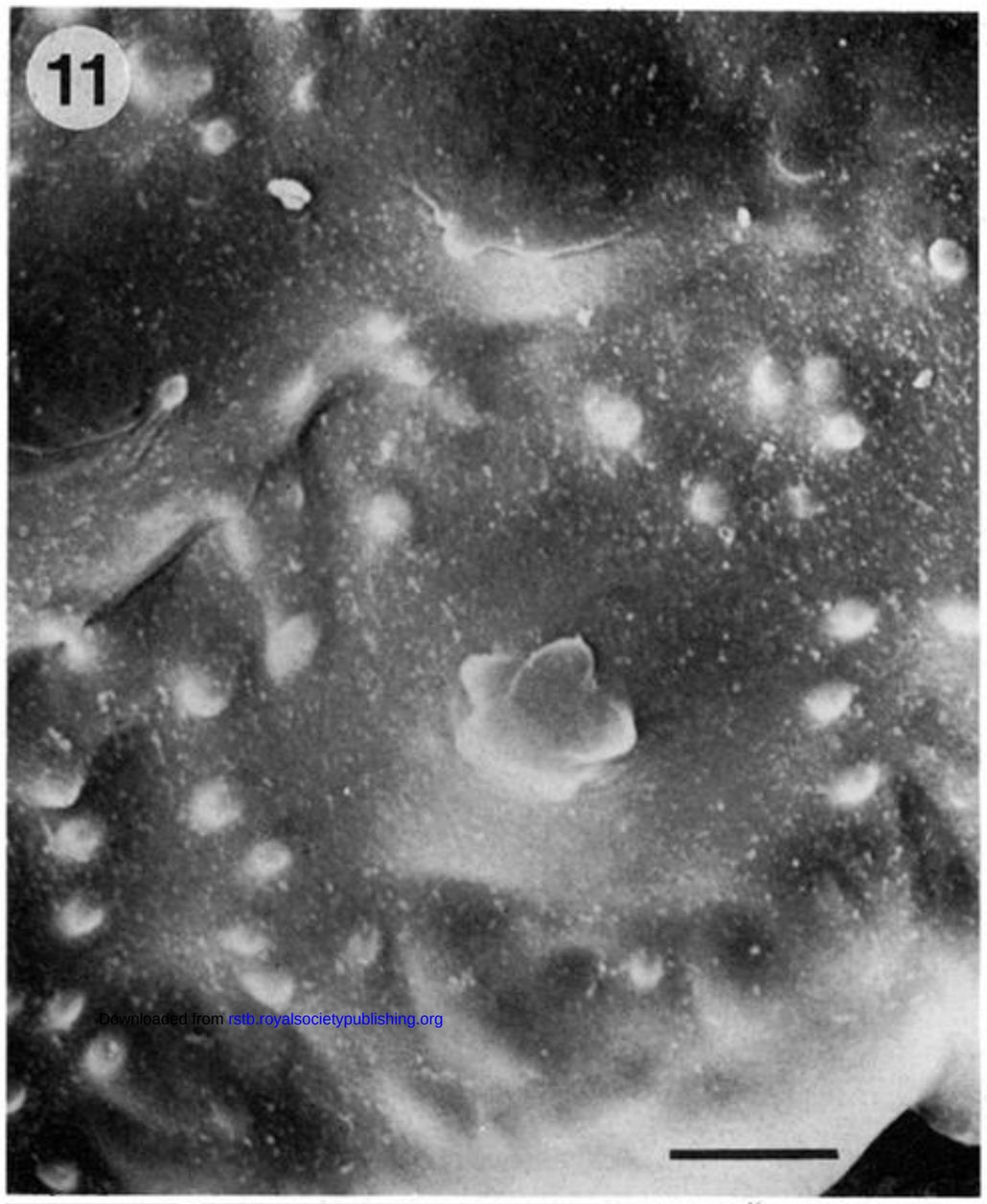


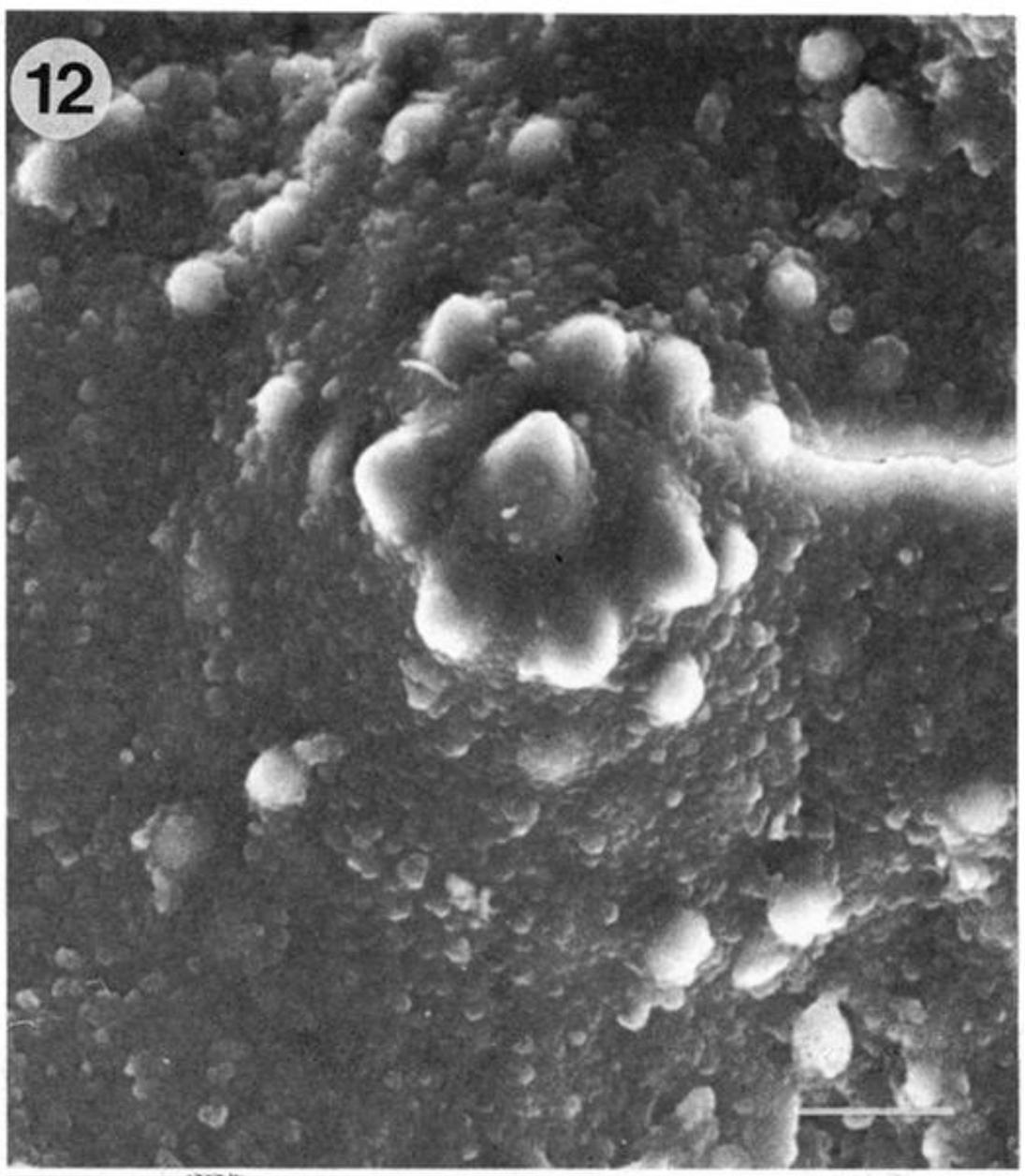




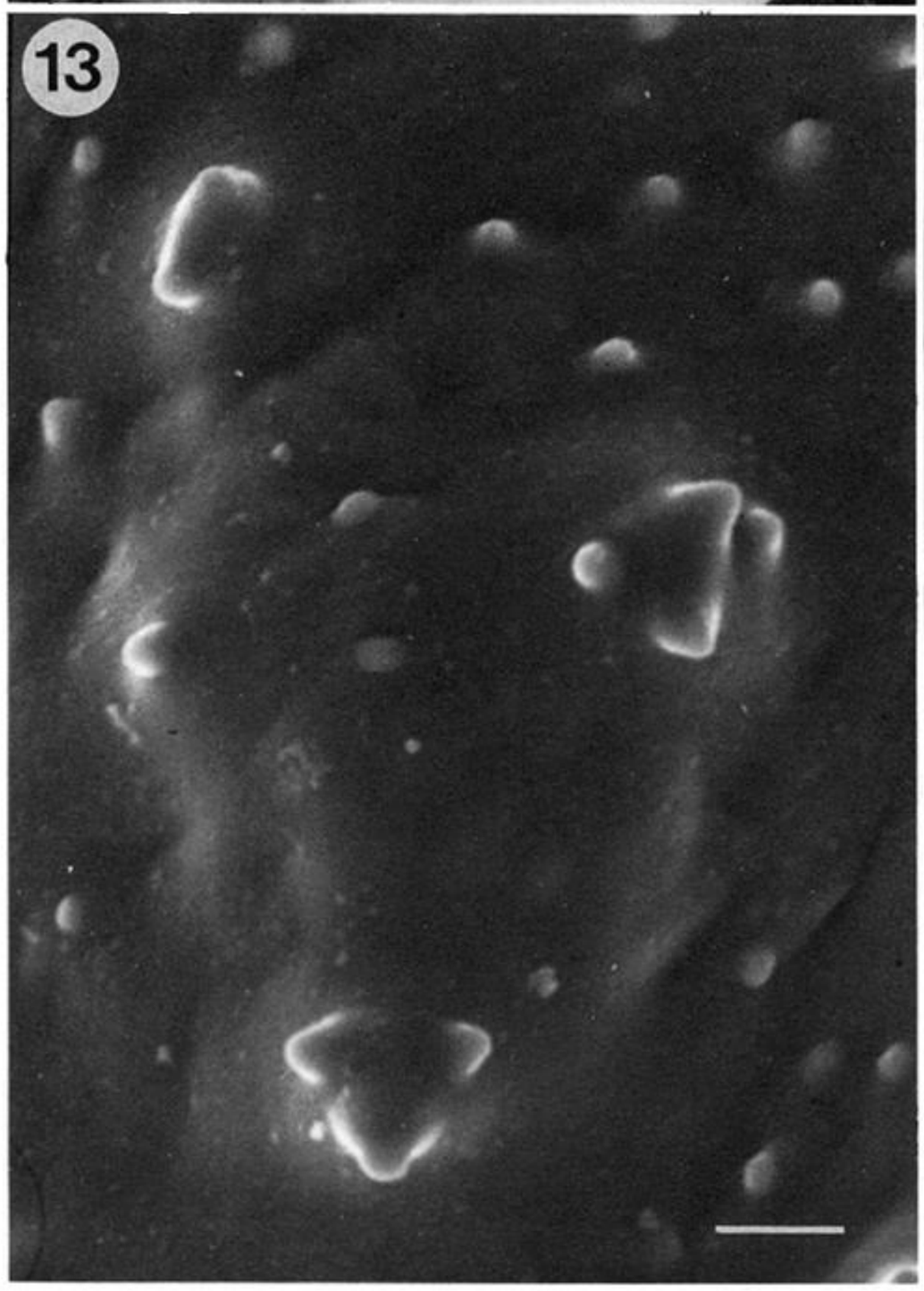


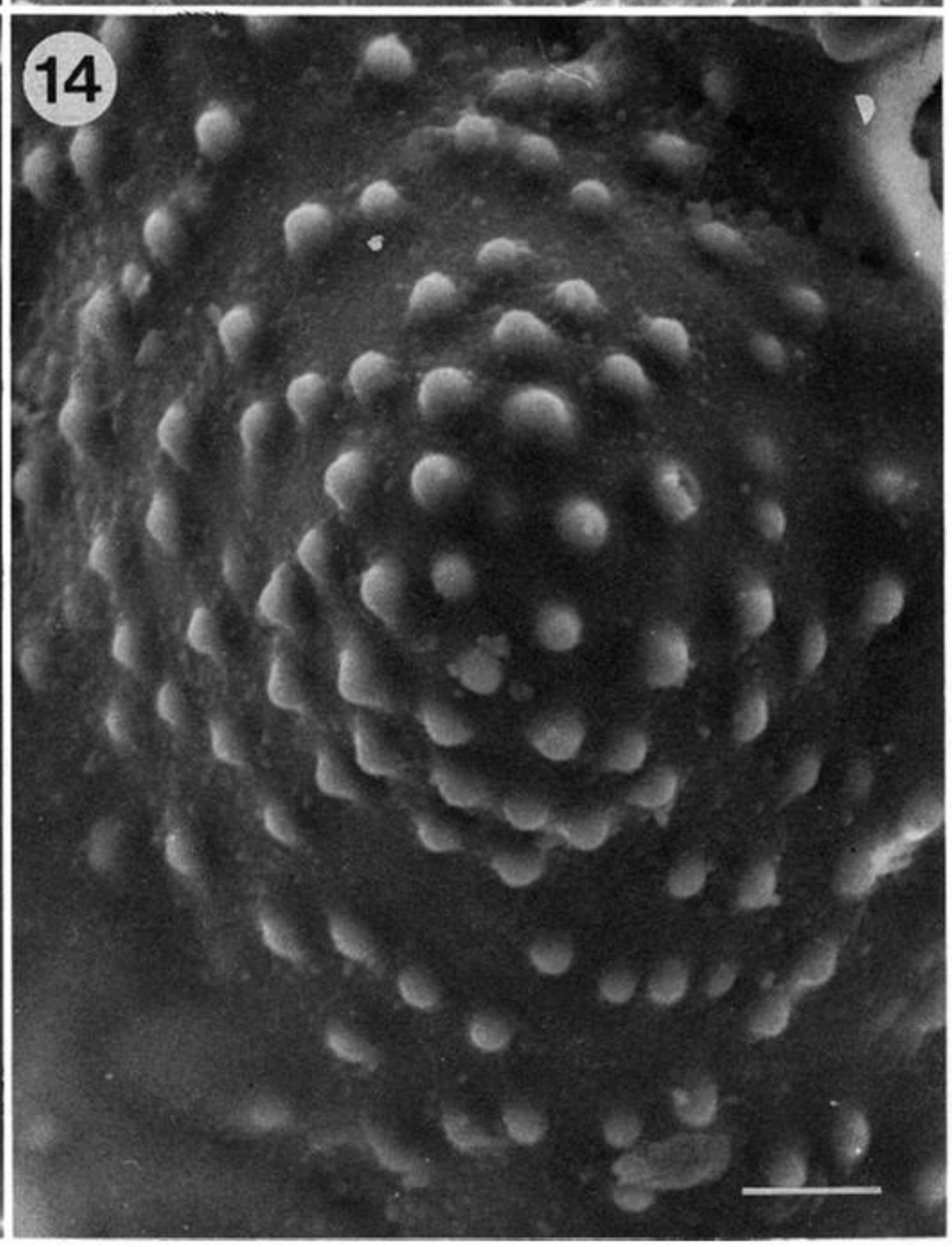




PHILOSOPHICAL TRANSACTIONS OF THE ROYAL SOCIETY B BIOLOGICAL SCIENCES

gures 11–14. Pilulae found in the groove flank region of the branches showing a range of cluster and star-like ggregates. Scale bars represent 1 μm.

igure 15. Fibrillar silica from a mature internode. The material is oriented with the principal axis of the plant.

igure 16. Fibrillar silica from an immature internode showing clear orientation and dense packing of the individual rils.

igure 17. Small regions of fibrillar material showing random orientation and some sheet-like silica.

igure 18. Silica from a node showing densely packed sheets of globular material.

igure 19. Immature node showing some particulate material and structurally indistinct beam-sensitive material.


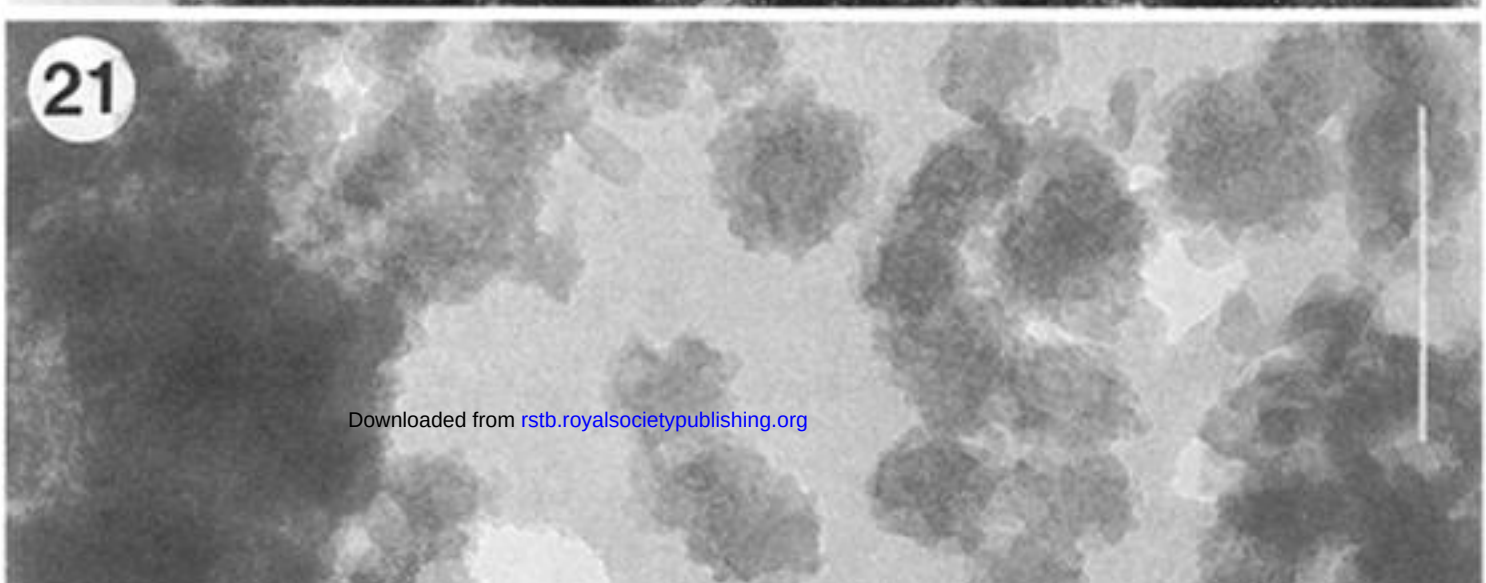




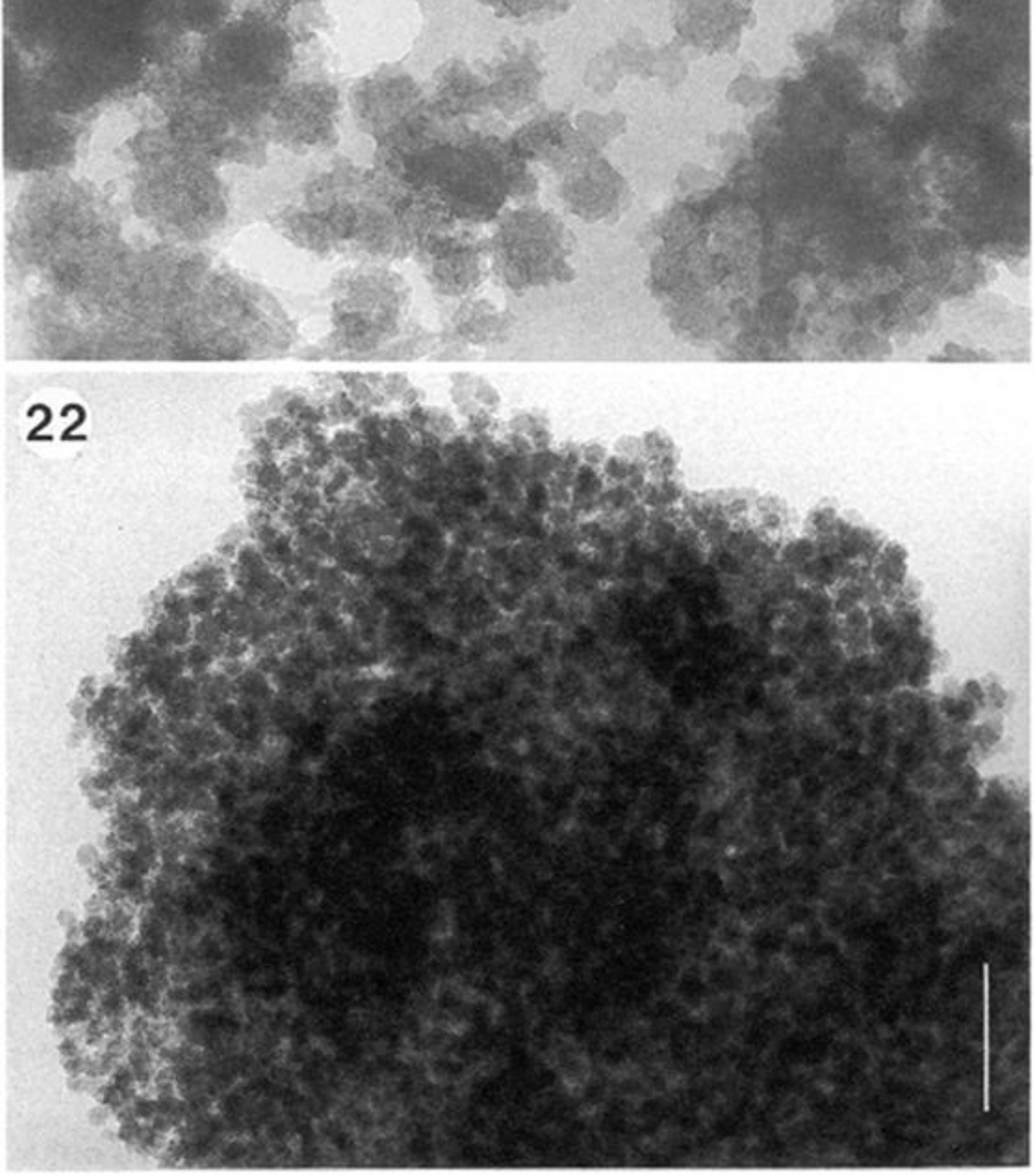


gure 20. Globular material and small areas of oriented terial (arrowed) from the branches.

gure 21. Beam-sensitive globular material from immature anches.

gure 22. Globular silica from the branches.